JACS
JOURNAL OF THE AMERICAN CHEMICAL SOCIETY
Article
pubs.acs.org/JACS

The Mechanism of a Ligand-Promoted C(sp^3)–H Activation and Arylation Reaction via Palladium Catalysis: Theoretical Demonstration of a Pd(II)/Pd(IV) Redox Manifold

Yanfeng Dang,[†] Shuanglin Qu,[†] John W. Nelson,[‡] Hai D. Pham,[‡] Zhi-Xiang Wang,*[,†,§] and Xiaotai Wang*[,‡]

[†]School of Chemistry and Chemical Engineering, University of the Chinese Academy of Sciences, Beijing 100049, China

[‡]Department of Chemistry, University of Colorado Denver, Campus Box 194, P.O. Box 173364, Denver, Colorado 80217-3364, United States

[§]Collaborative Innovation Center of Chemical Science and Engineering, Tianjin 300072, China

Supporting Information

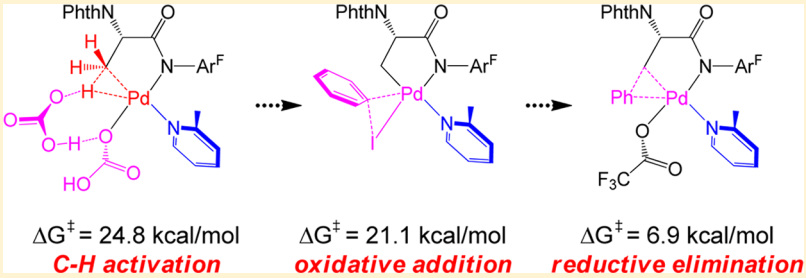

ABSTRACT: Density functional theory (DFT) computations (BP86 and M06-L) have been utilized to elucidate the detailed mechanism of a palladium-catalyzed reaction involving pyridine-type nitrogen-donor ligands that significantly expands the scope of C(sp^3)–H activation and arylation. The reaction begins with precatalyst initiation, followed by substrate binding to the Pd(II) center through an amidate auxiliary, which directs the ensuing bicarbonate-assisted C(sp^3)–H bond activation producing five-membered-ring cyclopalladate(II) intermediates. These Pd(II) complexes further undergo oxidative addition with iodobenzene to form Pd(IV) complexes, which proceed by reductive C–C elimination/coupling to give final products of arylation. The base-assisted C(sp^3)–H bond cleavage is found to be the rate-determining step, which involves hydrogen bond interactions. The mechanism unravels the intimate involvement of the added 2-picoline ligand in every phase of the reaction, explains the isolation of the cyclopalladate intermediates, agrees with the observed kinetic hydrogen isotope effect, and demonstrates the Pd(II)/Pd(IV) redox manifold.

1. INTRODUCTION

Palladium-catalyzed cross-coupling reactions using organohalides or other surrogates have been well developed over the past few decades.[1] These reactions constitute a useful methodology for constructing carbon–carbon and carbon–heteroatom bonds in organic synthesis. More recently, palladium-catalyzed tandem C–H activation and C–C coupling reactions have emerged, which allows creating new carbon–carbon bonds directly and economically from unactivated carbon–hydrogen bonds.[2,3] In the reactions reported earlier, the catalyst system frequently consists of a palladium salt (e.g., acetate) and additives such as silver carbonate, and the substrate contains an auxiliary directing group (e.g., 8-aminoquinoline or a weakly coordinating amide) that ligates with palladium and positions it near a particular C–H bond, so that the C–H bond activation step occurs through a five-membered-ring cyclopalladation pathway.[2d,m,4,5] The Yu group has recently advanced this method by adding N(sp^2)-donor ligands (e.g., 2-picoline) to the catalyst system.[6−10] This innovative approach, owing to the intimate ligand involvement, expands the scope of C(sp^3)–H bond activation and confers selectivity for primary or secondary C(sp^3)–H bonds.[7] For example, it has been applied in the synthesis of monoarylated alanines for peptide drug discovery, as well as unnatural chiral α-amino acids.[7]

This Article reports a detailed mechanism for this novel C(sp^3)–H activation reaction on the basis of DFT computational studies. We have chosen to compute the actual reaction that used the alanine-derived amide (**1a**) as a substrate (Scheme 1).[7] First, the reaction was optimized with the 2-picoline ligand (L) to achieve a high yield (up to 94%). Second, in the absence of the coupling partner iodobenzene, it produced the crystallographically characterized five-membered-ring cyclopalladation intermediates **A** and **A′** from a stoichiometric reaction,[11] with which computational results can

Received: December 4, 2014
Published: January 14, 2015

DOI: 10.1021/ja512374g
J. Am. Chem. Soc. 2015, 137, 2006−2014

Scheme 1. Pd-Catalyzed Ligand-Promoted C(sp^3)−H Arylation[a]

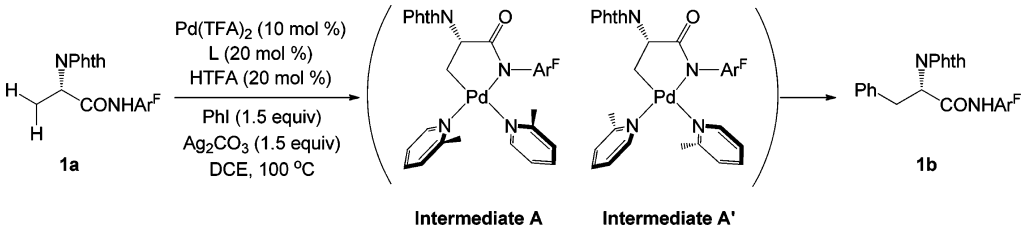

[a]TFA = Trifluoroacetate, L = 2-Picoline, Phth = Phthalimido, Ar^F = 4-$(CF_3)C_6F_4$, and DCE = 1,2-Dichloroethane.

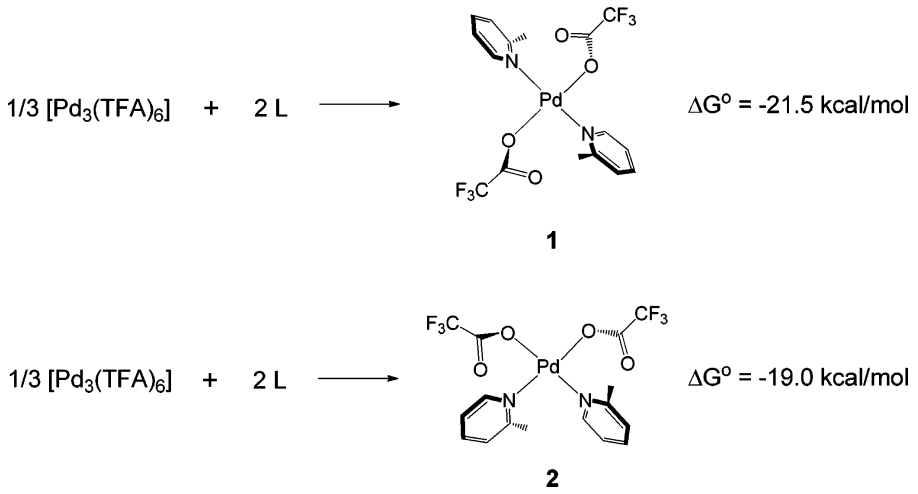

Figure 1. Formations of the most stable *trans*-$PdL_2(TFA)_2$ (**1**) and *cis*-$PdL_2(TFA)_2$ (**2**).

be checked. These intermediates not only were isolable but also were found to further react with iodobenzene to produce **1b**. This led the experimentalists to propose a Pd(II)/Pd(IV) pathway in which Pd(II) first activates the C(sp^3)−H bond to give a cyclopalladate(II) intermediate (e.g., **A**) that undergoes sequential oxidative addition by iodobenzene and reductive elimination to afford the final arylated product.[7] However, the detailed mechanism of this remarkable catalytic reaction has not been explored at the outset of this work. The present study constitutes a plausible mechanism that unravels the intimate ligand involvement, explains the isolation of intermediates **A** and **A′**, and demonstrates the Pd(II)/Pd(IV) catalytic cycle.

2. COMPUTATIONAL METHODS

Geometry optimizations and frequency calculations were performed at the BP86[12]/BS1 level in DCE solution using the SMD[13] solvation model with default convergence criteria, BS1 designating a mixed basis set of SDD[14] for palladium and iodine and 6-31G(d,p) for other atoms. Frequency outcomes were examined to confirm stationary points as minima (no imaginary frequencies) or transition states (only one imaginary frequency). Because the M06-L[15] functional includes noncovalent interactions and gives refined energies for organo-transition metal systems, we performed single-point energy calculations for all the BP86/BS1-optimized structures at the M06-L/BS2 level with solvation effects modeled by SMD in DCE solution, BS2 denoting a mixed basis set of SDD for palladium and iodine and 6-311++G(d,p) for other atoms. The BP86/BS1-calculated frequencies were used to obtain zero-point energy-corrected enthalpies and free energies at 298.15 K and 1 atm in DCE solution. Free energies (kcal/mol) obtained from the M06-L/BS2//BP86/BS1 calculations were used in the following discussion. All calculations were performed with Gaussian 09.[16]

3. RESULTS AND DISCUSSION

3.1. Initiation and Substrate Binding. The structures of intermediates **A** and **A′** suggest square planar Pd(II) bis-2-picoline complexes resulting from the initiation of the precatalyst $Pd(TFA)_2$,[17] for which we have considered both trans and cis geometries (Figure 1).[18] The formations of the trans and cis complexes **1** and **2** both have large thermodynamic driving forces. Thus, we do not rule out either of them at this stage and do consider both of them for subsequent reactions.

The alanine-derived substrate with the amide auxiliary can adopt several possible modes of coordination with palladium: as a charge-neutral N-donor amide (**1a**) or as a deprotonated N-donor amidate anion (**1a′**) or its resonance form, an O-donor imidate (**1a″**), as shown by eq 1. The deprotonation reaction

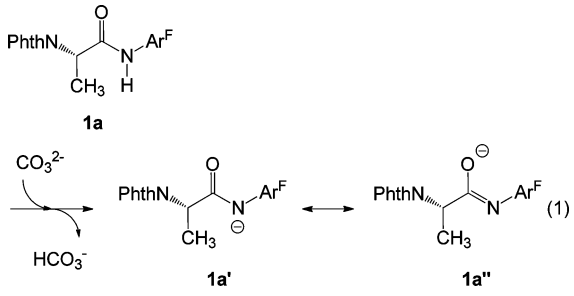

(eq 1) has a large driving force (ΔG° = −45.3 kcal/mol) that can be attributed to the electron-withdrawing effect of the $-Ar^F$ group; this would help shift the solubility equilibrium of Ag_2CO_3. We have considered all three coordination modes and found that the most favorable pathway involves the N-donor

DOI: 10.1021/ja512374g
J. Am. Chem. Soc. 2015, 137, 2006−2014

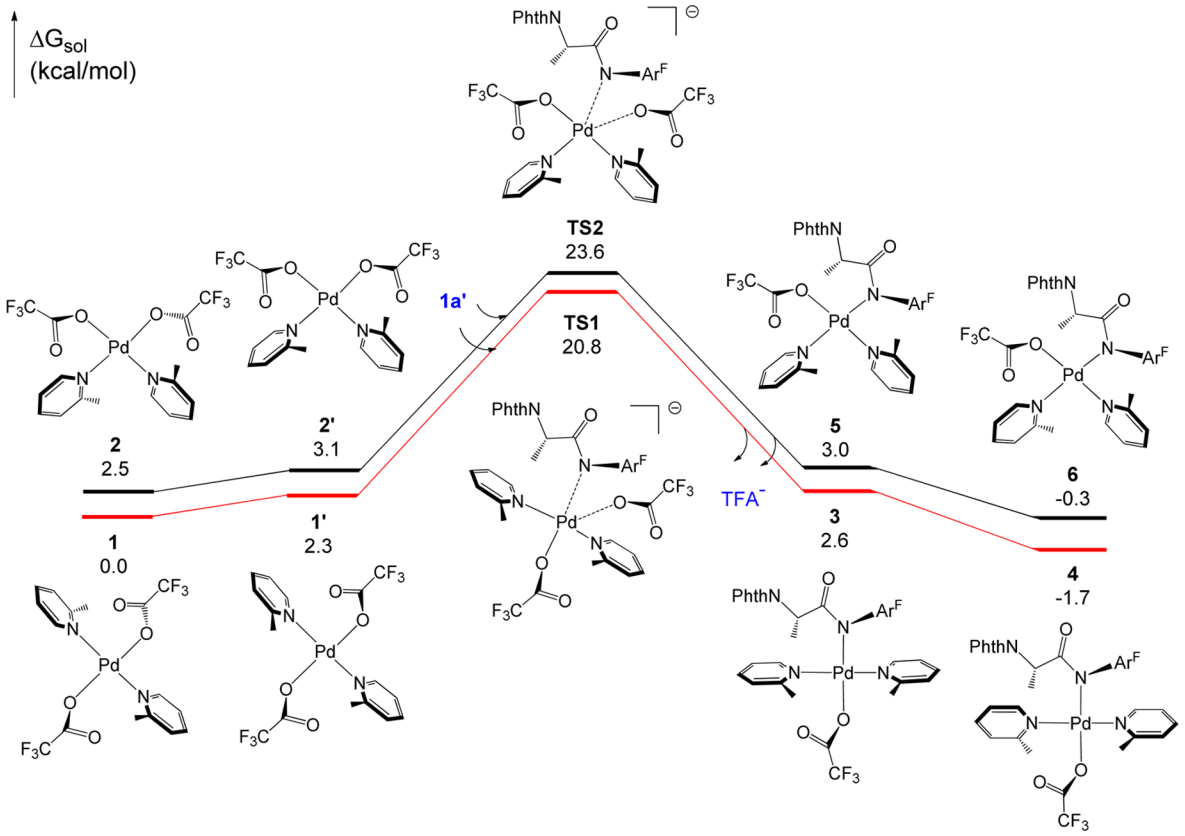

Figure 2. Free energy profiles for substitution reactions by **1a**′ starting from *trans*- and *cis*-$PdL_2(TFA)_2$ (**1** and **2**) and leading to **4** and **6**. Energies are relative to complex **1** and are mass balanced (similarly hereinafter).

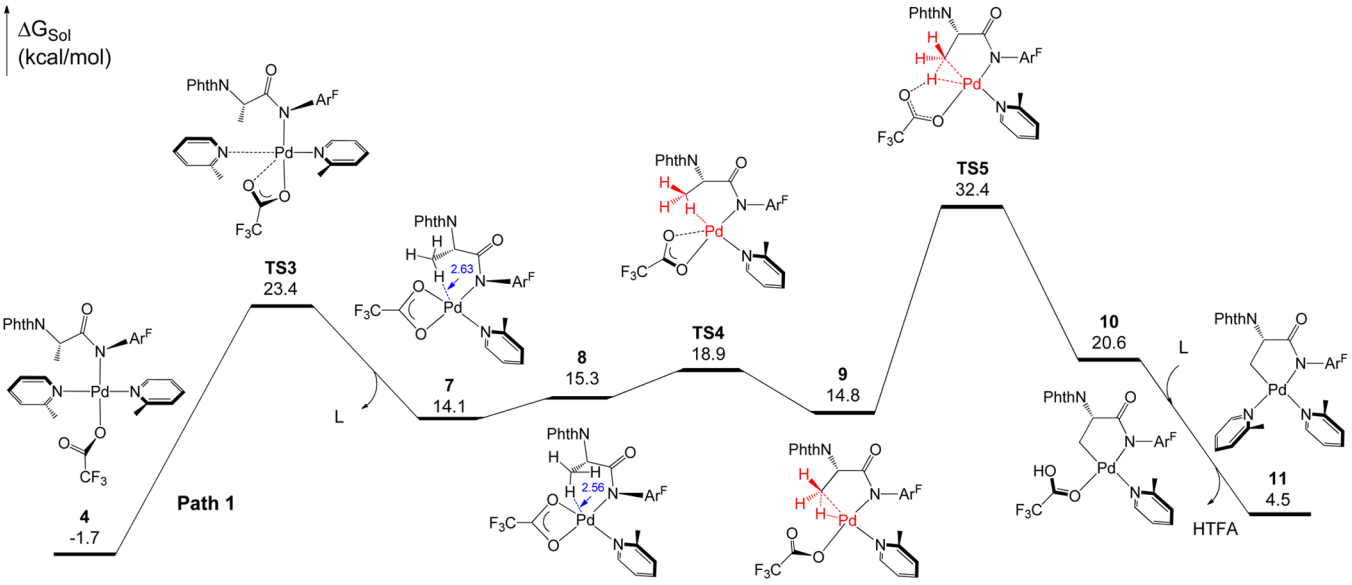

Figure 3. Free energy profile for the Pd(II)-catalyzed trifluoroacetate-assisted C(sp^3)–H bond activation leading to the cyclopalladation intermediate **A** (or **11**).

amidate **1a**′, which agrees with the Pd–N(amidate) coordination mode in the crystal structures of **A** and **A**′. This can be understood by considering that **1a**′ has a negative charge and its nitrogen donor atom has a stronger affinity for the Pd(II) center than the oxygen donor atom of **1a**″. We discuss the **1a**′-coordinating pathway here (Figure 2) and include the other less favorable modes of coordination in the Supporting Information (Figure S1).

As shown in Figure 2, complex **1** undergoes two consecutive rotations about the Pd–O and Pd–N dative bonds (Figure S2) to reach the conformation of **1**′ that has the least sterically hindered face for palladium to coordinate with **1a**′ through its amidate auxiliary. For the substitution of **1a**′, we located the interchange transition state **TS1** that proceeds to **3**. This substrate-binding step is thermodynamically and kinetically feasible, with ΔG° = 0.3 kcal/mol as well as an attainable

DOI: 10.1021/ja512374g
J. Am. Chem. Soc. 2015, 137, 2006–2014

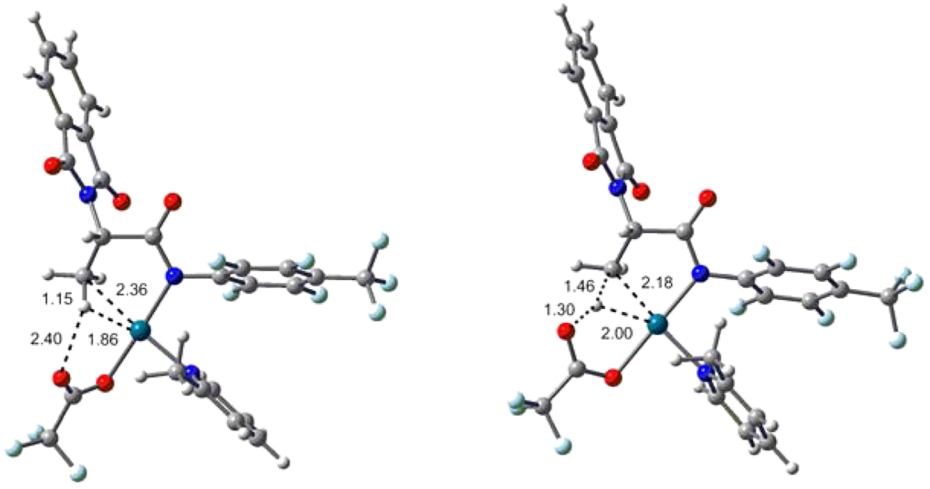

Figure 4. Optimized structures of **TS5** and its precursor complex **9**, with selected bond distances given in angstroms.

Scheme 2. Possible Pathways for Pd(II)-Catalyzed Bicarbonate-Assisted C(sp^3)−H Bond Activation, with Free Energies Given in kcal/mol[a]

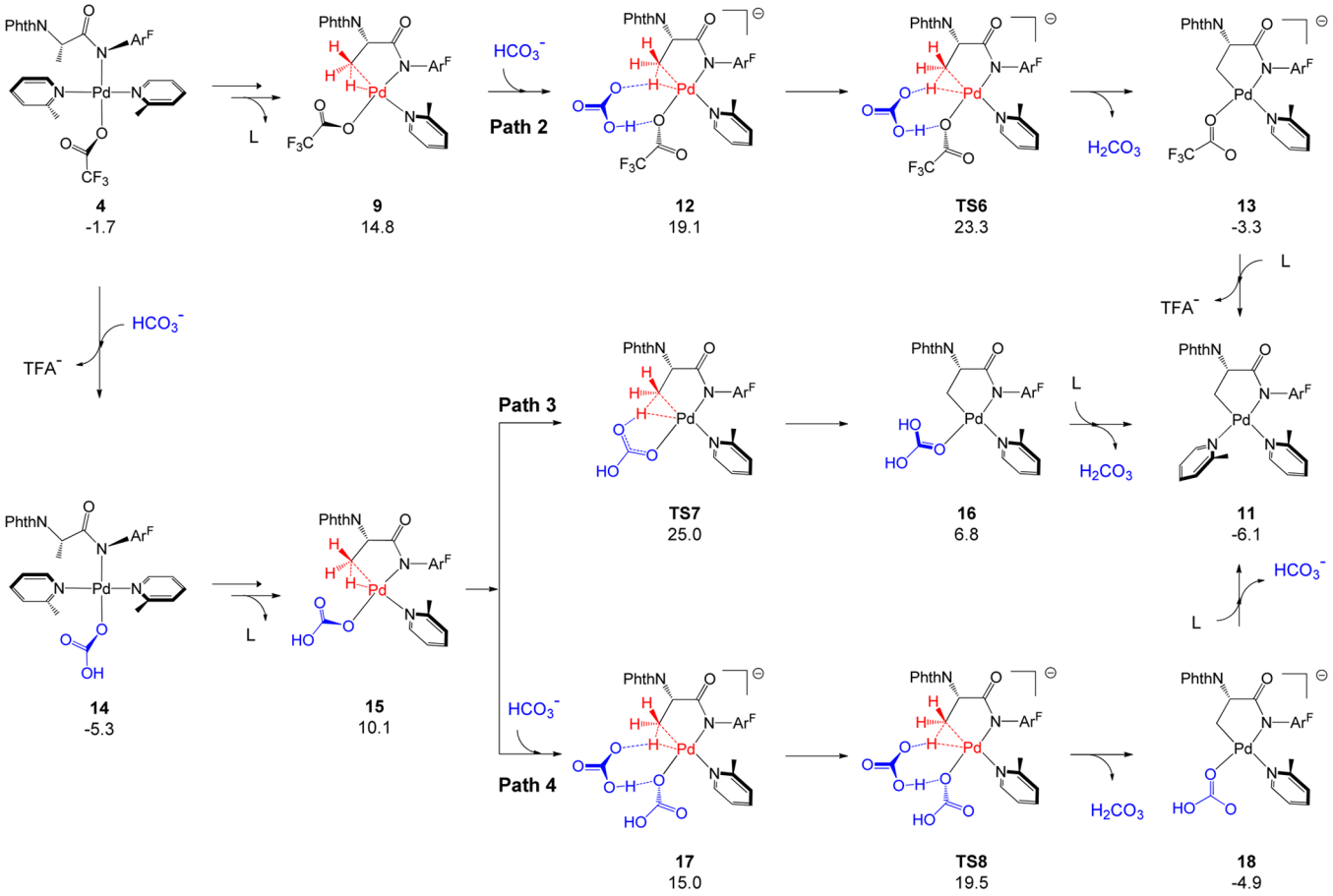

[a]The proton acceptor in paths 2−4 is bicarbonate, whereas it is trifluoroacetate in path 1. Thus, the relative energy of **11** (or intermediate **A**) in paths 2−4 is different from that in path 1 (see Figure 3).

activation free energy (18.5 kcal/mol). Complex **3** isomerizes through rotation of the Pd−N dative bond to afford the more stable conformer **4** in which the methyl groups of the 2-picoline ligands point away from each other to reduce steric repulsion. The conformation of **4** also facilitates the ensuing C(sp^3)−H bond cleavage (see below). The overall transformation from **1** to **4** is exergonic by 1.7 kcal/mol. The pathway starting from the less stable cis complex **2** and leading to complex **6** is completely analogous, with every corresponding intermediate or transition state at a higher-energy stationary point. As a

DOI: 10.1021/ja512374g
J. Am. Chem. Soc. 2015, 137, 2006−2014

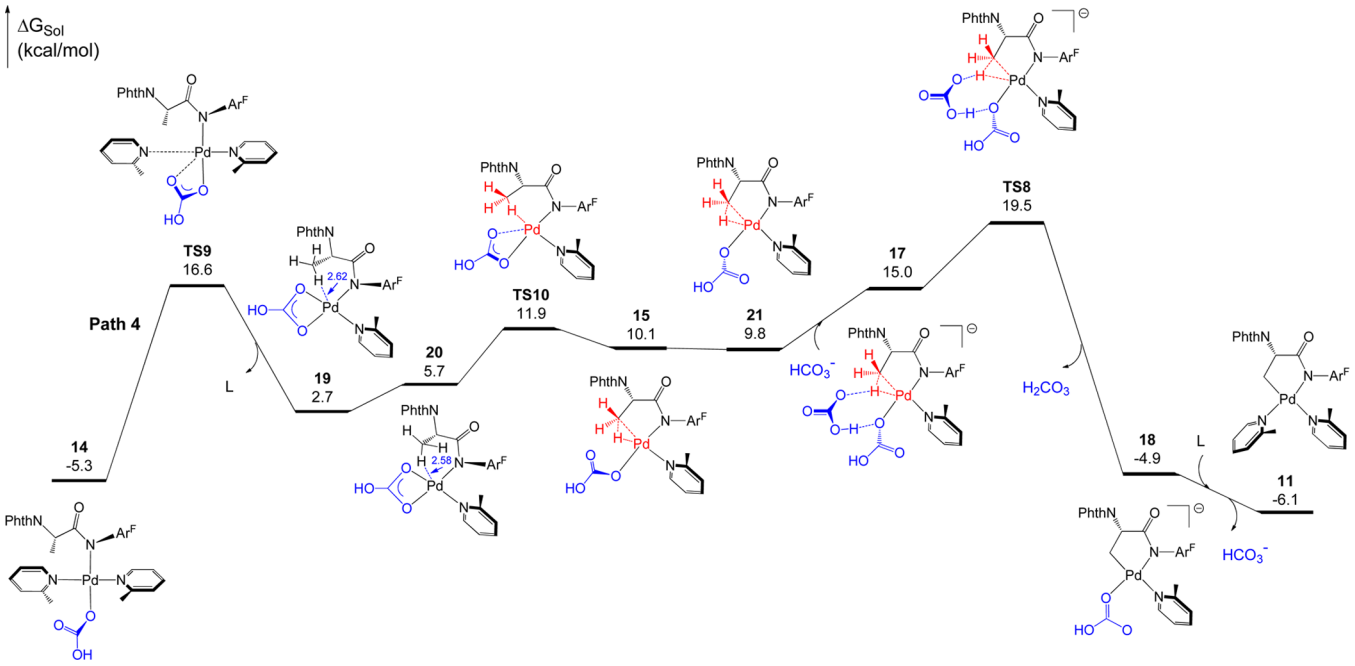

Figure 5. Free energy profile for the most favorable C(sp^3)−H bond activation pathway assisted by bicarbonate.

result, the formation of **6** is less favorable than the formation of **4**. Furthermore, complexes **4** and **6** would converge to the same bidentate carboxylate complex by releasing one 2-picoline ligand to facilitate the succeeding C−H activation (Figure S3). In the following sections, we will focus our discussion on the reaction pathways involving **4** as the active catalytic species.

3.2. C(sp^3)−H Bond Activation Assisted by Trifluoroacetate. Previous mechanistic studies on palladium carboxylate-catalyzed C(sp^2)/C(sp^3)−H activation have demonstrated the carboxylate-assisted concerted metalation−deprotonation (CMD) mechanism; that is, a coordinated carboxylate ion can act as an internal base to aid in cleaving the C−H bond via a six-membered-ring transition state.[19,20] Guided by this rationale, we located the reaction course from **4** to **9** via two consecutive intramolecular interchange substitutions (Figure 3).[21] First, complex **4** proceeds via **TS3** to the bidentate carboxylate complex **7**, with the dissociation of one 2-picoline ligand. Complex **7** then isomerizes through the rotation of the C(carbonyl)−C(α) bond to **8**. This moves the C(sp^3)−H bond being activated closer to the Pd(II) center to enable the second interchange step (see the distances in Å marked in **7** and **8**), in which the C(sp^3)−H bond undergoes agostic interaction with the Pd(II) center and displaces one carboxylate oxygen-donor atom via **TS4** to form complex **9**. The C(sp^3)−H bond becomes gradually activated during the **8** → **TS4** → **9** transformation, as indicated by the bond lengthening from 1.10 Å in **8** to 1.12 Å in **TS4** to 1.15 Å in **9**. The activated C(sp^3)−H bond in **9** facilitates the subsequent carboxylate-assisted CMD via **TS5** to cleave the C(sp^3)−H bond and form the five-membered-ring cyclopalladation complex **10** with a weakly bound neutral HTFA ligand. **TS5** is the highest stationary point and overall kinetic barrier in the pathway of the C(sp^3)−H bond activation. The optimized structures of **TS5** and its precursor **9** are shown in Figure 4.

Our calculations indicate that substitution of 2-picoline (L) for HTFA in **10**, along with the rotation of the Pd−N(picoline) dative bonds, theoretically could lead to four diastereomeric complexes with similar thermodynamic and kinetic preferences (Figure S4). Only two of them, namely **A** (or **11**) and **A′** (or **11′**), were actually isolated by crystallization from solution in the same crop. In intermediates **A** and **A′**, the 2-picoline methyl groups are oriented on the same side of the cyclopalladate ring, a conformation that can subject **A** and **A′** to stronger crystal packing forces. In other words, the four isomers interconvert in solution, but only **A** and **A′** crystallize into the solid phase because of stronger intermolecular attractive forces.

The reaction course from **4** to **TS5** to **10** consists of well-defined elementary steps occurring intramolecularly without added reagents (Figure 3), and as such, it has been evaluated to give an overall relative energy barrier of 34.1 kcal/mol (**TS5**−**4**). This kinetic barrier is somewhat too large to account for the high yield of the reaction. Because of the electron-withdrawing group $-CF_3$, trifluoroacetate is not strongly basic, which can explain the relatively high energy of **TS5**. Thus, the carboxylate-assisted path 1 might not be the most favorable pathway. These considerations led us to search for alternative, lower-energy C(sp^3)−H bond activation pathways involving stronger bases.

3.3. C(sp^3)−H Bond Activation Assisted by Bicarbonate. In the reaction mixture, there exists the bicarbonate ion (another base) in significant quantities, which arises mostly from the eq 1 reaction.[22] Thus, we have considered the bicarbonate-assisted C(sp^3)−H activation and computed three additional deprotonation pathways (Scheme 2).[23]

In path 2, complex **4** proceeds to **9** in several steps that have already been characterized (see Figure 3). Complex **9** then hydrogen bonds with bicarbonate to form **12**, which facilitates the succeeding bicarbonate-assisted deprotonation via **TS6** to cleave the C(sp^3)−H bond. Alternatively, complex **4** can proceed by substitution of bicarbonate for trifluoroacetate to form **14**, which is exergonic by 3.6 kcal/mol. Complex **14** converts to **15** via two consecutive intramolecular substitutions (see Figure 5 below), at which point the reaction bifurcates onto paths 3 and 4. Paths 3 and 4 have the controlling transition states of C−H bond cleavage **TS7** and **TS8**, respectively. **TS6**, **TS7**, and **TS8** are all lower in energy than **TS5** of path 1 (see Figure 3), which can be rationalized by

DOI: 10.1021/ja512374g
J. Am. Chem. Soc. 2015, 137, 2006−2014

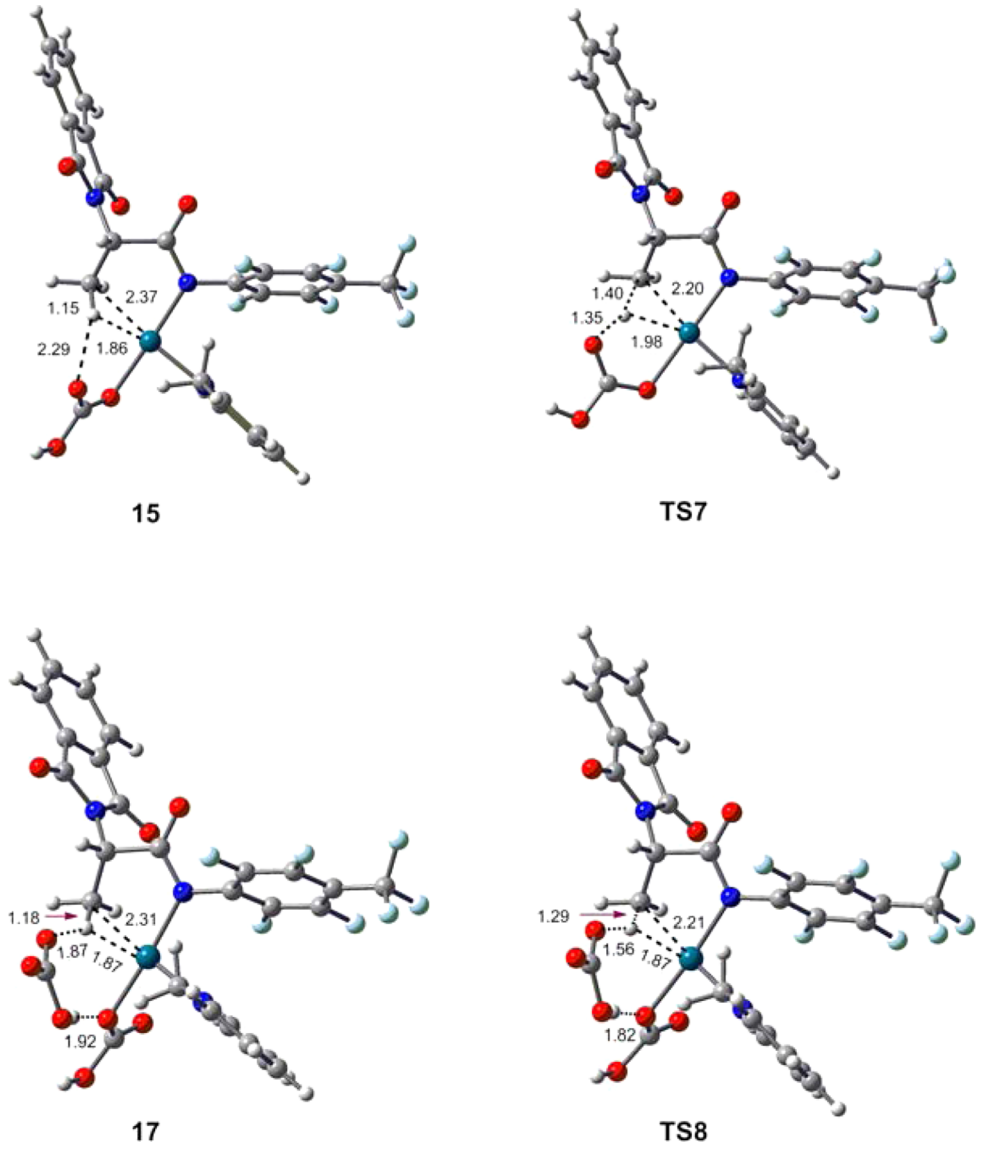

Figure 6. Optimized structures of **TS7** and **TS8** and their immediate precursors **15** and **17**, with selected bond distances given in angstroms.

considering that bicarbonate is a stronger base than trifluoroacetate. Of **TS6**, **TS7**, and **TS8**, **TS8** has the lowest energy, indicating path 4 to be the most favorable C(sp^3)−H activation pathway, which is presented in more detail below (Figure 5).

As shown in Figure 5, the transformation of **14** to **15** through two consecutive interchange substitutions is similar to the transformation of **4** to **9** in path 1 (see Figure 3), except that the trifluoroacetate ligand is replaced with bicarbonate. Complex **15** then undergoes the Pd−O(bicarbonate) dative bond rotation to become **21**, a conformation that can accommodate another bicarbonate ion to form the hydrogen-bonded complex **17**. Deprotonation of the C(sp^3)−H bond occurs within **17** via **TS8** to form the five-membered-ring cyclopalladation complex **18** with the release of carbonic acid. Substitution of 2-picoline for the bicarbonate ligand in **18** can generate intermediate **A** (or **11**). The energy barrier **TS8** is 24.8 kcal/mol relative to complex **14**, which is considerably lower than the corresponding energy barrier (**TS5**, $\Delta G^{\ddagger}$ = 34.1 kcal/mol) in path 1. Furthermore, the transformation from **1** to **A** (or **11**) via path 4 is exergonic by 6.1 kcal/mol, as opposed to path 1 that is endergonic by 4.1 kcal/mol.

Now we explain the relative order of energy for the rate-determining barriers **TS6** (path 2), **TS7** (path 3), and **TS8** (path 4). Structurally, **TS6** and **TS8** bear close similarities, and the only difference is between the ligated trifluoroacetate in the former and bicarbonate in the latter (see Scheme 2). Because of the greater electron density on the oxygen-donor atoms, bicarbonate has a stronger affinity for the Pd(II) center than does trifluoroacetate, which stabilizes **TS8** relative to **TS6**. What makes **TS8** more stable than **TS7** is less evident, but an examination of the optimized geometries of **TS7** and **TS8** and their precursor complexes **15** and **17** reveals some important influences (Figure 6). In complex **17**, the hydrogen bonding interaction at 1.87 Å between the bicarbonate oxygen and the C(sp^3)−H hydrogen appears to be crucial. First, it brings the oxygen atom closer to the hydrogen atom for the subsequent proton transfer. Second, it weakens the C(sp^3)−H bond further and stretches it to 1.18 Å, as compared with the corresponding C(sp^3)−H bond at 1.15 Å in complex **15**. In addition, the

DOI: 10.1021/ja512374g
J. Am. Chem. Soc. 2015, 137, 2006−2014

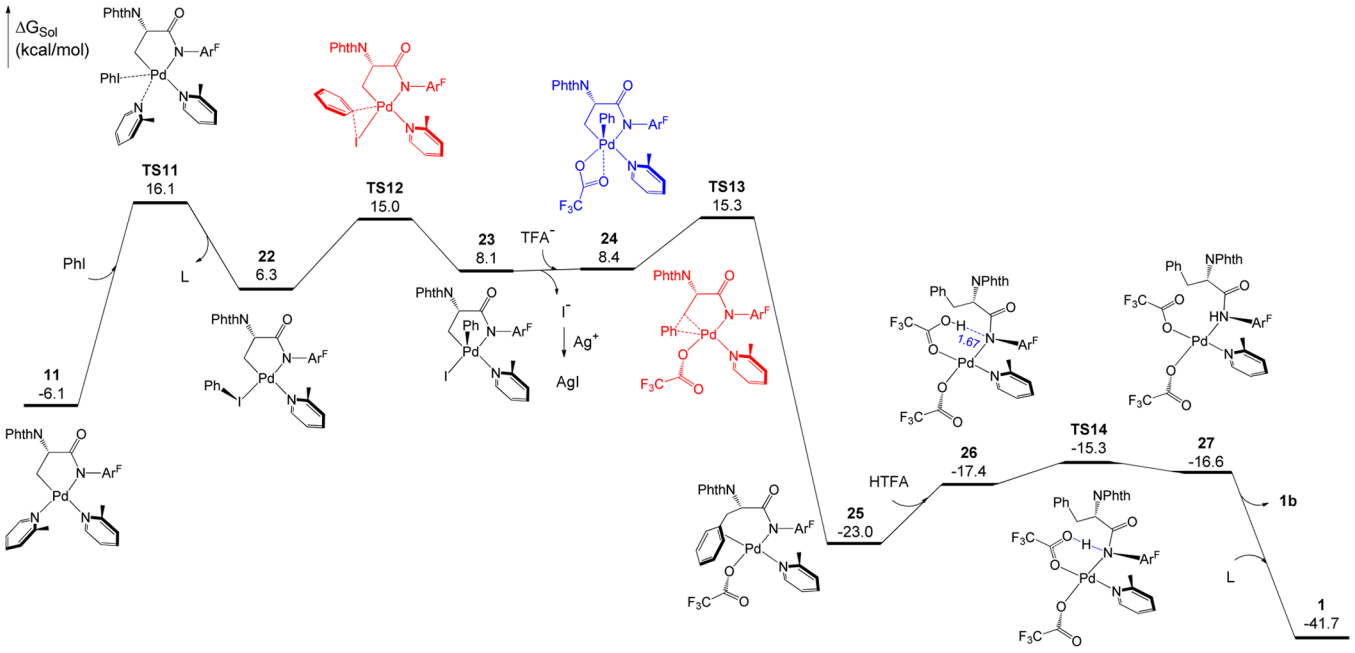

Figure 7. Free energy profile for the reaction of complex **11** with PhI leading to the product **1b**.

hydrogen bond at 1.82 Å between the two bicarbonate ions in **TS8** helps lower this energy barrier.

To our knowledge, the kinds of hydrogen bonding interactions in **TS8** and its precursor complex **17** have not been explored by previous studies on C−H activation catalyzed by palladium carboxylates with base additives. The closest structures that have been reported are computed transition states in which a bicarbonate ion acts as a base on a C−H bond intermolecularly.[20d,h] We have also located intermolecular transition states resembling **TS8** but lacking hydrogen bonds, which are higher in energy than **TS8** (Figure S6). Thus, the hydrogen bonds in **17** and **TS8** have a differentiating effect on the stability of **TS8**. In summary, for the C(sp^3)−H bond activation leading to the cyclopalladate(II) intermediates (**A** and **A′**), our computational analysis has established the bicarbonate-assisted path 4 as the most favorable pathway with the rate-determining barrier **TS8**.

3.4. Oxidative Addition and Carbon−Carbon Reductive Coupling. The Pd(II)/Pd(IV) redox manifold has previously been proposed in organometallic reactions.[2d,4,24−26] Specifically, the oxidations of Pd(II) to Pd(IV) by MeI and PhI have been deliberated in the literature, with the former putatively characterized by X-ray crystallography[27] and the latter proposed in catalytic cycles.[5b,f] We have computed a Pd(II)/Pd(IV) pathway involving the oxidative addition of the Pd(II) complex **11** by PhI and leading to the final arylated product **1b**, as shown in Figure 7. Complex **11** undergoes substitution of PhI for 2-picoline via **TS11** to form **22**, which brings the Ph−I bond into contact with the palladium(II) center to facilitate the ensuing oxidative addition (OA). The OA step via **TS12** has an attainable activation energy of 8.7 kcal/mol and produces the five-coordinate Pd(IV) complex **23**.[28] We next considered the abstraction of iodide from **23** by silver(I) and computed complex **24** in the presence of the trifluoroacetate ligand. Complex **24** then undergoes reductive elimination at the Pd(IV) center via **TS13** to form a new carbon−carbon bond and complete the β-arylation of the alanine-derived substrate.[29] The resulting Pd(II) complex **25** contains a Pd−η^2-phenyl bond, fulfilling a 16-electron valence shell on the Pd(II) center. The Pd−η^2-phenyl coordination mode has previously been computed for Pd(II) complexes.[30−32] It is also worth noting that the reductive elimination step is highly exergonic by 31.4 kcal/mol. The reaction course from **11** to **25** constitutes a redox cycle between the Pd(II) and Pd(IV) oxidation states (see Figure 7), with intermediates and transition states that are structurally and energetically plausible. It represents a rare example of theoretical demonstration for the Pd(II)/Pd(IV) redox manifold in a palladium-catalyzed C−C coupling reaction using a simple alkyl/aryl halide (RX) as the oxidant.

It might seem trivial protonating the amidate ligand in complex **25** to give the final product **1b**, but we computed a plausible pathway (Figure S8), with the key components shown in Figure 7. Complex **26** brings the acidic H atom proximal to the coordinated amidate N atom at a hydrogen bond distance of 1.67 Å. The ensuing proton transfer to the N atom via **TS14** is facile, resulting in complex **27** with the product **1b** weakly bound to the Pd(II) center through the neutral amide auxiliary. Substitution of 2-picoline for **1b** in complex **27** can release **1b** and regenerate the active catalyst **1**.

For the complete catalytic cycle (Figures 2, 5, and 7), the Pd(II)-catalyzed bicarbonate-assisted C(sp^3)−H bond cleavage in path 4 is the rate-determining step with the kinetic barrier **TS8** that is 24.8 kcal/mol relative to **14**. The reaction course from **14** to **17** to **TS8** consists of well-defined elementary steps, and as such, it has been evaluated to give the turnover-limiting barrier that is more plausible than otherwise defined. This overall activation energy (24.8 kcal/mol) would be readily available at the experimental temperature (100 °C), thereby accounting for the high yield of the reaction shown in Scheme 1.[7] In addition, the computationally characterized rate-determining step agrees with the observation of the kinetic hydrogen isotope effect (k_H/k_D = 8.1) indicating that the actual rate-determining step involves breaking a C−H bond.[7] On another note, we also computed the pathway for the reaction of

DOI: 10.1021/ja512374g
J. Am. Chem. Soc. 2015, 137, 2006−2014

intermediate **A′** with iodobenzene (Figure S9), which is analogous to that of intermediate **A** shown in Figure 7.

4. CONCLUSION

In conclusion, we have utilized DFT calculations to elucidate the detailed mechanism of a newly developed ligand-promoted C(sp^3)−H activation and arylation reaction on a Pd(II)/Pd(IV) catalytic cycle. The proposed mechanism involves substitution of the alanine-derived substrate through the amidate auxiliary, bicarbonate-assisted C(sp^3)−H bond activation, oxidative addition of Pd(II) to Pd(IV) by iodobenzene, and reductive C−C elimination/coupling to give the final product of arylation. The added 2-picoline ligand is involved in every stage, as well as in the initiation of the precatalyst, which apparently stabilizes the intermediates and transition states. The C(sp^3)−H bond cleavage is found to be the rate-determining step, which involves heretofore unexplored hydrogen bond interactions. The proposed mechanism explains the isolation of the intermediate complexes of cyclopalladation, as well as the observed kinetic hydrogen isotope effect. Taken together, the computational results demonstrate rich experimental−theoretical synergy.

■ ASSOCIATED CONTENT

Supporting Information

Additional computational results, energies, and Cartesian coordinates of the optimized structures. This material is available free of charge via the Internet at http://pubs.acs.org.

■ AUTHOR INFORMATION

Corresponding Authors

*zxwang@ucas.ac.cn

*xiaotai.wang@ucdenver.edu

Notes

The authors declare no competing financial interest.

■ ACKNOWLEDGMENTS

We acknowledge support for this work by the National Science Foundation of China (Grant Nos. 21173263 and 21373216) and the University of Colorado Denver. A proportion of the computational work was performed using the Extreme Science and Engineering Discovery Environment (XSEDE), which is supported by National Science Foundation Grant Number ACI-1053575. We greatly appreciate the insightful suggestions of the anonymous reviewers which helped us to improve the study.

■ REFERENCES

(1) Selected reviews: (a) Stille, J. K. *Angew. Chem., Int. Ed. Engl.* **1986**, *25*, 508. (b) Miyaura, N.; Suzuki, A. *Chem. Rev.* **1995**, *95*, 2457. (c) Demeijere, A.; Meyer, F. E. *Angew. Chem., Int. Ed. Engl.* **1995**, *33*, 2379. (d) Beletskaya, I. P.; Cheprakov, A. V. *Chem. Rev.* **2000**, *100*, 3009. (e) Luh, T.-Y.; Leung, M.-K.; Wong, K.-T. *Chem. Rev.* **2000**, *100*, 3187. (f) Trost, B. M.; Crawley, M. L. *Chem. Rev.* **2003**, *103*, 2921. (g) *Metal-Catalyzed Cross-Coupling Reactions*, 2nd ed.; de Meijere, A., Diedrich, F., Eds.; Wiley-VCH: Weinheim, Germany, 2004. (h) Surry, D. S.; Buchwald, S. L. *Angew. Chem., Int. Ed.* **2008**, *47*, 6338. (i) Martin, R.; Buchwald, S. L. *Acc. Chem. Res.* **2008**, *41*, 1461. (j) Hartwig, J. F. *Nature* **2008**, *455*, 314. (k) Xue, L.; Lin, Z. *Chem. Soc. Rev.* **2010**, *39*, 1692. (l) Seechurn, C. C. C. J.; Kitching, M. O.; Colacot, T. J.; Sniekus, V. *Angew. Chem., Int. Ed.* **2012**, *51*, 5062. (m) García-Melchor, M.; Braga, A. A. C.; Lledós, A.; Ujaque, G.; Maseras, F. *Acc. Chem. Res.* **2013**, *46*, 2626.

(2) Selected reviews on transition-metal-catalyzed C−H bond activation reactions: (a) Alberico, D.; Scott, M. E.; Lautens, M. *Chem. Rev.* **2007**, *107*, 174. (b) Seregin, I. V.; Gevorgyan, V. *Chem. Soc. Rev.* **2007**, *36*, 1173. (c) Davies, H. M. L.; Manning, J. R. *Nature* **2008**, *451*, 417. (d) Chen, X.; Engle, K. M.; Wang, D. H.; Yu, J. Q. *Angew. Chem., Int. Ed.* **2009**, *48*, 5094. (e) Daugulis, O.; Do, H.-Q.; Shabashov, D. *Acc. Chem. Res.* **2009**, *42*, 1074. (f) Ackermann, L.; Vicente, R.; Kapdi, A. R. *Angew. Chem., Int. Ed.* **2009**, *48*, 9792. (g) Lyons, T. W.; Sanford, M. S. *Chem. Rev.* **2010**, *110*, 1147. (h) Yeung, C. S.; Dong, V. M. *Chem. Rev.* **2011**, *111*, 1215. (i) Engle, K. M.; Mei, T.-S.; Wasa, M.; Yu, J.-Q. *Acc. Chem. Res.* **2012**, *45*, 788. (j) Yamaguchi, J.; Yamaguchi, A. D.; Itami, K. *Angew. Chem., Int. Ed.* **2012**, *51*, 8960. (k) Neufeldt, S. R.; Sanford, M. S. *Acc. Chem. Res.* **2012**, *45*, 936. (l) Ackermann, L. *Acc. Chem. Res.* **2014**, *47*, 281. (m) Noisier, A. F. M.; Brimble, M. A. *Chem. Rev.* **2014**, *114*, 8775.

(3) (a) Leow, D.; Li, G.; Mei, T.-S.; Yu, J.-Q. *Nature* **2012**, *486*, 518. (b) Tang, R.; Li, G.; Yu, J.-Q. *Nature* **2014**, *507*, 215. (c) Chan, K. S. L.; Wasa, M.; Chu, L.; Laforteza, B. N.; Miura, M.; Yu, J.-Q. *Nat. Chem.* **2014**, *6*, 146. (d) Liu, Y.-J.; Xu, H.; Kong, W.-J; Shang, M.; Dai, H.-X.; Yu, J.-Q. *Nature* **2014**, *515*, 389.

(4) Rouquet, G.; Chatani, N. *Angew. Chem., Int. Ed.* **2013**, *52*, 11726.

(5) (a) Giri, R.; Chen, X.; Yu, J.-Q. *Angew. Chem., Int. Ed.* **2005**, *44*, 2112. (b) Zaitsev, V. G.; Shabashov, D.; Daugulis, O. *J. Am. Chem. Soc.* **2005**, *127*, 13154. (c) Reddy, B. V. S.; Reddy, L. R.; Corey, E. J. *Org. Lett.* **2006**, *8*, 339. (d) Wang, D.-H.; Wasa, M.; Giri, R.; Yu, J.-Q. *J. Am. Chem. Soc.* **2008**, *130*, 7190. (e) Wasa, M.; Engle, K. M.; Yu, J.-Q. *J. Am. Chem. Soc.* **2009**, *131*, 9886. (f) Tran, L. D.; Daugulis, O. *Angew. Chem., Int. Ed.* **2012**, *51*, 5188. (g) Zhang, S.-Y.; Li, Q.; He, G.; Nack, W. A.; Chen, G. *J. Am. Chem. Soc.* **2013**, *135*, 12135.

(6) Wasa, M.; Chan, K. S. L.; Zhang, X.-G.; He, J.; Miura, M.; Yu, J.-Q. *J. Am. Chem. Soc.* **2012**, *134*, 18570.

(7) He, J.; Li, S.; Deng, Y.; Fu, H.; Laforteza, B. N.; Spangler, J. E.; Homs, A.; Yu, J.-Q. *Science* **2014**, *343*, 1216.

(8) Li, S.; Chen, G.; Feng, C.-G; Gong, W.; Yu, J.-Q. *J. Am. Chem. Soc.* **2014**, *136*, 5267.

(9) Deng, Y.; Gong, W.; He, J.; Yu, J.-Q. *Angew. Chem., Int. Ed.* **2014**, *53*, 6692.

(10) Zhu, R.-Y.; He, J.; Wang, X.-C.; Yu, J.-Q. *J. Am. Chem. Soc.* **2014**, *136*, 13194.

(11) Only intermediate **A** was presented in the main text of ref 7. The crystallographic information file (CCDC-985676) deposited in the Cambridge Crystallographic Data Centre clearly shows a mixture of **A** and **A′**.

(12) (a) Becke, A. D. J. *Chem. Phys.* **1993**, *98*, 1372. (b) Becke, A. D. J. *Chem. Phys.* **1993**, *98*, 5648. (c) Perdew, J. P.; Chevary, J. A.; Vosko, S. H.; Jackson, K. A.; Pederson, M. R.; Singh, D. J.; Fiolhais, C. *Phys. Rev. B* **1993**, *48*, 4978. (d) Perdew, J. P. *Phys. Rev. B* **1986**, *33*, 8822.

(13) Marenich, A. V.; Cramer, C. J.; Truhlar, D. G. *J. Phys. Chem. B* **2009**, *113*, 6378.

(14) (a) Andrae, D.; Häussermann, U.; Dolg, M.; Stoll, H.; Preuss, H. *Theor. Chim. Acta* **1990**, *77*, 123. (b) Dolg, M.; Wedig, U.; Stoll, H.; Preuss, H. *J. Chem. Phys.* **1987**, *86*, 866.

(15) (a) Zhao, Y.; Truhlar, D. G. *Theor. Chem. Acc.* **2008**, *120*, 215. (b) Zhao, Y.; Truhlar, D. G. *Acc. Chem. Res.* **2008**, *41*, 157. (c) Kulkarni, A. D.; Truhlar, D. G. *J. Chem. Theory Comput.* **2011**, *7*, 2325. (d) Zhao, Y.; Truhlar, D. G. *J. Chem. Theory Comput.* **2009**, *5*, 324.

(16) Frisch, M. J.; Trucks, G. W.; Schlegel, H. B.; Scuseria, G. E.; Robb, M. A.; Cheeseman, J. R.; Scalmani, G.; Barone, V.; Mennucci, B.; Petersson, G. A.; Nakatsuji, H.; Caricato, M.; Li, X.; Hratchian, H. P.; Izmaylov, A. F.; Bloino, J.; Zheng, G.; Sonnenberg, J. L.; Hada, M.; Ehara, M.; Toyota, K.; Fukuda, R.; Hasegawa, J.; Ishida, M.; Nakajima, T.; Honda, Y.; Kitao, O.; Nakai, H.; Vreven, T.; Montgomery, J. A., Jr.; Peralta, J. E.; Ogliaro, F.; Bearpark, M.; Heyd, J. J.; Brothers, E.; Kudin, K. N.; Staroverov, V. N.; Kobayashi, R.; Normand, J.; Raghavachari, K.; Rendell, A.; Burant, J. C.; Iyengar, S. S.; Tomasi, J.; Cossi, M.; Rega, N.; Millam, N. J.; Klene, M.; Knox, J. E.; Cross, J. B.; Bakken, V.; Adamo, C.; Jaramillo, J.; Gomperts, R.; Stratmann, R. E.; Yazyev, O.; Austin, A. J.; Cammi, R.; Pomelli, C.; Ochterski, J. W.; Martin, R. L.;

DOI: 10.1021/ja512374g
J. Am. Chem. Soc. 2015, 137, 2006−2014

Morokuma, K.; Zakrzewski, V. G.; Voth, G. A.; Salvador, P.; Dannenberg, J. J.; Dapprich, S.; Daniels, A. D.; Farkas, Ö.; Foresman, J. B.; Ortiz, J. V.; Cioslowski, J.; Fox, D. J. *Gaussian 09, revision A.01*; Gaussian, Inc.: Wallingford, CT, 2009.

(17) Trinuclear $[Pd_3(TFA)_6]$ was optimized on the basis of the single crystal structure reported in the following reference: Batsanov, A. S.; Timko, G. A.; Struchkov, Yu. T.; Gerbeleu, N. V.; Indrichan, K. M.; Popovich, G. A. *Koord. Khim. (Russ.) (Coord. Chem.)* **1989**, *15*, 688.

(18) We also considered the formation of $[PdL_2(\kappa^2\text{-TFA})]^+$ with bidentate TFA coordination, which proved to be much less favorable thermodynamically than those of **1** and **2** (by at least 24.1 kcal/mol). Thus, $[PdL_2(\kappa^2\text{-TFA})]^+$ was not considered further.

(19) (a) Lapointe, D.; Fagnou, K. *Chem. Lett.* **2010**, *39*, 1118. (b) Balcells, D.; Clot, E.; Eisenstein, O. *Chem. Rev.* **2010**, *110*, 749. (c) Ackermann, L. *Chem. Rev.* **2011**, *111*, 1315. (d) Ackermann, L. *Acc. Chem. Res.* **2014**, *47*, 281. (e) Musaev, D. G.; Figg, T. M.; Kaledin, A. L. *Chem. Soc. Rev.* **2014**, *43*, 5009.

(20) (a) Davies, D. L.; Donald, S. M. A.; Macgregor, S. A. *J. Am. Chem. Soc.* **2005**, *127*, 13754. (b) Lafrance, M.; Fagnou, K. *J. Am. Chem. Soc.* **2006**, *128*, 16496. (c) García-Cuadrado, D.; Braga, A. A. C.; Maseras, F.; Echavarren, A. M. *J. Am. Chem. Soc.* **2006**, *128*, 1066. (d) García-Cuadrado, D.; de Mendoza, P.; Braga, A. A. C.; Maseras, F.; Echavarren, A. M. *J. Am. Chem. Soc.* **2007**, *129*, 6880. (e) Lafrance, M.; Gorelsky, S. I.; Fagnou, K. *J. Am. Chem. Soc.* **2007**, *129*, 14570. (f) Gorelsky, S. I.; Lapointe, D.; Fagnou, K. *J. Am. Chem. Soc.* **2008**, *130*, 10848. (g) Rousseaux, S.; Gorelsky, S. I.; Chung, B. K. W.; Fagnou, K. *J. Am. Chem. Soc.* **2010**, *132*, 10692. (h) Tang, S.-Y.; Guo, Q.-X.; Fu, Y. *Chem.—Eur. J.* **2011**, *17*, 13866. (i) Zhang, S.; Shi, L.; Ding, Y. *J. Am. Chem. Soc.* **2011**, *133*, 20218. (j) Musaev, D. G.; Kaledin, A.; Shi, B.-F.; Yu, J.-Q. *J. Am. Chem. Soc.* **2012**, *134*, 1690. (k) Giri, R.; Lan, Y.; Liu, P.; Houk, K. N.; Yu, J.-Q. *J. Am. Chem. Soc.* **2012**, *134*, 14118. (l) Sanhueza, I. A.; Wagner, A. M.; Sanford, M. S.; Schoenebeck, F. *Chem. Sci.* **2013**, *4*, 2767. (m) Yang, Y.-F.; Cheng, G.-J.; Liu, P.; Leow, D.; Sun, T.-Y.; Chen, P.; Zhang, X.; Yu, J.-Q.; Wu, Y.-D.; Houk, K. N. *J. Am. Chem. Soc.* **2014**, *136*, 344. (n) Cheng, G.-J.; Yang, Y.-F.; Liu, P.; Chen, P.; Sun, T.-Y.; Li, G.; Zhang, X.; Houk, K. N.; Yu, J.-Q.; Wu, Y.-D. *J. Am. Chem. Soc.* **2014**, *136*, 894. (o) Anand, M.; Sunoj, R. B.; Schaefer, H. F., III. *J. Am. Chem. Soc.* **2014**, *136*, 5535.

(21) With both 2-picoline ligands attached to palladium, no pathways of cyclopalladation could be found leading to **11** probably due to steric crowding around the palladium center.

(22) The additive trifluoroacetic acid (HTFA) is present only in 20% mol, so its reaction with Ag_2CO_3 could not be a major source of bicarbonate.

(23) We also considered the $C(sp^3)$–H bond activation assisted by the other bases that occur in the reaction mixture. These pathways, however, would all involve higher energy barriers compared to path 4 (see Figure S5 in the Supporting Information for more details).

(24) Hickman1, A. J.; Sanford, M. S. *Nature* **2012**, *484*, 177.

(25) Dick, A. R.; Kampf, J. W.; Sanford, M. S. *J. Am. Chem. Soc.* **2005**, *127*, 12790.

(26) (a) Ball, N. D.; Gary, J. B.; Ye, Y.; Sanford, M. S. *J. Am. Chem. Soc.* **2011**, *133*, 7577. (b) Powers, D. C.; Lee, E.; Ariafard, A.; Sanford, M. S.; Yates, B. F.; Canty, A. J.; Ritter, T. *J. Am. Chem. Soc.* **2012**, *134*, 12002. (c) Lotz, M. D.; Remy, M. S.; Lao, D. B.; Ariafard, A.; Yates, B. F.; Canty, A. J.; Mayer, J. M.; Sanford, M. S. *J. Am. Chem. Soc.* **2014**, *136*, 8237.

(27) Byers, P. K.; Canty, A. J.; Skelton, B. W.; White, A. H. *J. Chem. Soc., Chem. Commun.* **1986**, 1722.

(28) We also considered the oxidative addition pathways involving silver(I) coordination with iodobenzene through iodine, whose kinetic barriers are comparable to those of **TS12** in energy (see Figure S7 in the Supporting Information for more details).

(29) We also considered the reductive elimination from **23** with iodine as the ligand (see Figure S13 in the Supporting Information for details), which has a higher kinetic barrier (**TS26-s**) compared to **TS13** with trifluoroacetate as the ligand.

(30) Albert, K.; Gisdakis, P.; Rösch, N. *Organometallics* **1998**, *17*, 1608.

(31) Lee, M.-T.; Lee, H. M.; Hu, C.-H. *Organometallics* **2007**, *26*, 1317.

(32) Dang, Y.; Qu, S.; Wang, Z.-X.; Wang, X. *J. Am. Chem. Soc.* **2014**, *136*, 986.

DOI: 10.1021/ja512374g
J. Am. Chem. Soc. 2015, 137, 2006–2014